CONFERENCES AND SYMPOSIA

75th ANNIVERSARY OF IZMIRAN

Some aspects of magnetosphere–ionosphere relations

A A Petrukovich, M M Mogilevsky, A A Chernyshov, D R Shklyar

Contents

Abstract. This paper reviews the characteristics of plasma-wave perturbations produced by wave-particle interactions in the magnetosphere–ionosphere system. These perturbations may, notably, be due to lightning discharges and to radiation from high-power low-frequency transmitters. These can form wave-guide channels, i.e., density inhomogeneities, which originate in the ionosphere above the radiation source and extend along geomagnetic field lines in the magnetosphere. Although different in nature, the natural and man-made radiation sources may have similar effects on processes in the circumterrestrial plasma, causing the excitation of a variety of emissions in it and stimulating the precipitation of charged particles from the magnetosphere into the ionosphere.

Keywords: magnetosphere–ionosphere connection, low-frequency emissions, active experiments, lightning discharges, wave–particle interactions, particle heating and precipitation

1. Introduction

The study of magnetosphere–ionosphere connection is of great interest and importance both for fundamental physics, expanding our knowledge about processes in magnetoactive plasma, and for solving practical problems related to navigation, communication, radar, and radio astronomy.

The magnetosphere is a region in near-Earth space, where plasma behavior is controlled by the Earth magnetic field.

A A Petrukovich, M M Mogilevsky, A A Chernyshov, D R Shklyar
Space Research Institute, Russian Academy of Sciences,
ul. Profsoyuznaya 84/32, 117997 Moscow, Russian Federation
E-mail: apetruko@iki.rssi.ru, mogilevsky@romance.iki.rssi.ru,
        achernyshov@iki.rssi.ru, david@iki.rssi.ru

Due to the flow of the solar wind (SW) around Earth's magnetosphere, a magnetic cavity is formed, with its size determined by the dynamic equilibrium of the SW plasma kinetic pressure and the magnetic pressure of the Earth field. As the SW pressure increases, the size of the magnetosphere decreases, its plasma density increases, and the excess plasma is pushed along the magnetic field into the ionosphere. The decrease in the SW pressure leads to an increase in the magnetosphere volume, which becomes filled with the ionospheric plasma.

In this way, the ionosphere is the plasma 'reservoir' for the magnetosphere, and vice versa. Therefore, in order to adequately describe large-scale, global processes in the circumterrestrial plasma, one needs to consider the magnetosphere–ionosphere system as a whole, despite the difference between plasma properties in the ionosphere and magnetosphere. The description of small-scale local processes also needs to consider the magnetosphere–ionosphere system as a whole. In this case, the plasma dynamics are governed mostly by various electrostatic and electromagnetic oscillations and waves, which can be easily excited in the magnetoactive plasma and undergo strong damping [1].

Besides the inner sources of waves in plasma — instabilities — an important role in the magnetosphere–ionosphere system's dynamics is played by external sources. These can be either natural, for example, lightning discharges during thunderstorm activity [2, 3], or artificial (anthropogenic), for example, the radiation of short-wave heating facilities [4–11] and strong low-frequency (LF) emitters [12].

The interaction of high-power radio waves with the magnetosphere–ionosphere system causes the formation of regions with an increased density of charged particles. These regions group into plasma inhomogeneities — ducts — which stretch thousands and tens of thousands of kilometers in the magnetosphere along the magnetic field. These inhomogeneities are waveguides for whistler waves and play a key role in the propagation of low-frequency waves in the magnetosphere.

Both natural and anthropogenic forms of radiation, despite their different nature and sources, can have a similar influence on processes in the near-Earth plasma. These are the questions that will be discussed in this paper.

The layout of the paper is as follows. In Section 2 we analyze the waves which are excited by the lightning discharges and are related to ion cyclotron and whistler modes. Their role in the particle precipitation from the magnetosphere to the ionosphere is discussed. Section 3 deals with the results of active experiments, based on direct measurements of the plasma characteristics and electromagnetic radiation properties, measured aboard spacecraft. Some unsolved problems and their possible solutions are discussed in Section 4.

2. Lightning discharge radiation in magnetosphere–ionosphere connection

Lightning discharges with a duration from several dozen microseconds to several milliseconds, which occur on Earth's surface with an average frequency of 10^{-7} km^{-2} s^{-1} [13, 14], are the source of a broadband electromagnetic radiation. This radiation, according to the modern conception, propagates in the Earth–ionosphere waveguide and partially penetrates into the ionosphere and magnetosphere, where it propagates as ion-cyclotron and whistler waves. One of the main mechanisms of magnetosphere–ionosphere connection lies in the interaction of these waves with the charged particles of the ionosphere and magnetosphere, which leads both to the precipitation of particles from magnetosphere to the ionosphere [2] and to the heating of ionosphere ions due to the absorption of the waves [3]. This mechanism and related issues will be briefly discussed in Sections 2.1, 2.2.

2.1 Wave packets excited by lightning discharges in the upper ionosphere and magnetosphere

The frequency range of waves that are excited by lightning discharges and that have a large enough intensity in the upper ionosphere and magnetosphere extends from several hundred hertz to several hundred kilohertz [15, 16]. Certainly, this frequency range is not determined by the lightning discharge duration and strongly depends on the problem geometry and dispersive characteristics of the medium.

The problem of defining the spectrum width of excited radiation can be qualitatively solved in the following way. In Earth's atmosphere, radiation propagates up to the lower boundary of the ionosphere at a speed close to the speed of light, but its speed becomes significantly lower in the ionosphere, where the refractive index rapidly increases.

It is clear that after the lightning discharge ends, by the time of the 'last' horizontally propagating beam reaches the lower boundary of the ionosphere, all the emission of the lightning discharge will be concentrated there. Since the lower ionosphere height h is significantly smaller than Earth's radius R_{E}, the vertical dimension l_{n} of the region occupied by radiation is much smaller than its horizontal dimension. Therefore, if we expand the ionosphere disturbance into the Fourier integral, the dominant components will be the ones with the wave vectors directed almost vertically and their characteristic values are $k_{\mathrm{n}} \gtrsim 1/l_{\mathrm{n}}$. The frequency band of the radiation can now be defined as that corresponding to a frequency band $\omega(k_{\mathrm{n}})$, where $\omega = \omega(\mathbf{k})$ is the dispersion relation in the ionosphere.

Experiment and calculations confirm that waves excited by lightning discharges correspond to ion-cyclotron and whistler modes [17, 18]. Further in this section we will discuss the whistler waves in the magnetosphere. The role of ion-cyclotron waves in the ionosphere–magnetosphere connection was discussed in paper [3]. At the 'initial moment', the electromagnetic field disturbance in the upper ionosphere, caused by lightning discharge, can be represented as wave packets (with the characteristic wave vectors, mentioned above) that are localized in the region with dimensions which are much smaller than Earth's radius. Obviously, this disturbance has a broad spatial spectrum. However, far enough away from this region and, correspondingly, after a long time the radiation can be represented as the wave packet with a slowly varying frequency and a wave vector, which occur at a specific instant of time at a given point.

2.2 Resonant interaction of whistler waves with charged particles in the magnetosphere

As the calculated results show [19], in the absence of ducts (density perturbations that are localized near the geomagnetic field line of force and can be a kind of a waveguide for whistler waves), in the near-equatorial region, where the electron–wave interaction is most effective, the whistler wave enters the quasiresonant propagation regime in which the angle θ between the wave vector and the external magnetic field is close to the resonant cone angle: $\cos\theta \simeq \omega/\omega_{\mathrm{ce}}$ (in the standard notation). In this case, the refractive index $N = kc/\omega$ of the wave greatly increases and the wave becomes quasielectrostatic, with its electric field directed almost along the wave vector and the magnetic field $B \ll NE$ (in the CGS system of units). After the wave reaches the equator and during its propagation in the hemisphere, opposite to that of lightning discharge, the wave refractive index continues to increase, which makes it possible for the wave to resonantly interact with protons at high cyclotron resonances. The quasi-electrostatic wave is linearly polarized, which allows us to consider its resonant interaction with electrons and protons in the same way. (Clearly, the interaction specifics, mostly related to the different ratio between the wave frequency and the particle gyrofrequency, remain in force).

The field of the quasielectrostatic wave packet can be written out in the form

$$\mathbf{E}(\mathbf{r}, t) = -\nabla\Phi(\mathbf{r}, t)\,, \quad \Phi(\mathbf{r}, t) = \Phi_0(\mathbf{r}, t)\sin\Psi(\mathbf{r}, t)\,, \qquad (1)$$

while the local wave vector $\mathbf{k}(\mathbf{r}, t)$ and the local frequency $\omega(\mathbf{r}, t)$ are defined by the relations

$$\mathbf{k}(\mathbf{r}, t) = \frac{\partial\Psi}{\partial\mathbf{r}}\,, \quad \omega(\mathbf{r}, t) = -\frac{\partial\Psi}{\partial t}\,.$$

Due to the azimuthal symmetry of the problem and vertical direction of the initial wave vectors, the waves propagate in the meridional plane, and the equations of particle motion have a first integral x_0, which is a transverse (relative to the external magnetic field) coordinate of the particle's guiding center in the meridional plane. At the same time, the equations of particle motion can be written down in the Hamiltonian form with canonical variables: $(p_\parallel, z)$ — longitudinal momentum and longitudinal coordinate, and (μ, φ), where φ is the particle gyrophase, and μ is its magnetic

moment

$$\mu = \frac{mv_\perp^2}{2\Omega} \,.$$

Here, m is the particle's mass ($m = m_e$ for electrons, and $m = m_i$ for protons), and $\Omega = eB_0/mc$ is the absolute value of the gyrofrequency for the appropriate type of a particle. The transverse coordinate of the particle can be expressed through the canonical variables mentioned above in the following way:

$$x = x_0 + \frac{v_\perp}{\Omega} \sin\varphi \equiv x_0 + \sqrt{\frac{2\mu}{m\Omega}} \sin\varphi \,,$$

and the Hamiltonian takes the form

$$H(p_\parallel, z, \mu, \varphi, t) = \frac{p_\parallel^2}{2m} + \mu\,\Omega(z) + q\Phi(z, \mu, \varphi, t)\,, \qquad (2)$$

where $q = e$ and $q = -e$ for protons and electrons, respectively. Under the condition that the gyroradius of the particle be much less than the inhomogeneity scale, the phase of the field is defined by the following expression

$$\Psi = \Psi_0(z, t) + k_\perp(x - x_0) \equiv \Psi_0(z, t) + \lambda \sin\varphi \,,$$

where λ is the dimensionless Larmor radius:

$$\lambda = \frac{k_\perp v_\perp}{\Omega} \equiv k_\perp \sqrt{\frac{2\mu}{m\Omega}} \,.$$

At the same time, the local longitudinal wave vector and the local frequency are determined from the relations

$$k_\parallel \simeq \frac{\partial\Psi_0}{\partial z}\,, \quad \omega \simeq -\frac{\partial\Psi_0}{\partial t} \,.$$

The Hamiltonian expansion into the Fourier series in terms of φ in the new variables assumes the form

$$H(p_\parallel, z, \mu, \varphi, t) = \frac{p_\parallel^2}{2m} + \mu\,\Omega(z)$$
$$+ q\Phi_0(z, t) \sum_n J_n(\lambda) \sin\left(\Psi_0(z, t) + n\varphi\right)\,, \qquad (3)$$

where J_n are the Bessel functions of the nth order.

By setting the full derivative of $\Psi_0(z, t) + n\varphi$ equal to zero along the particle trajectory, we can find the condition of resonant wave–particle interaction:

$$k_\parallel(z, t)\,v_\parallel - \omega(z, t) + n\Omega(z) = 0\,,$$
$$\text{or} \quad v_\parallel = v_{\text{res}\,n} \equiv \frac{\omega - n\Omega}{k_\parallel}\,, \qquad (4)$$

where it is taken into account that, according to formula (3), $\mathrm{d}\varphi/\mathrm{d}t \simeq \Omega$.

2.2.1 Isolated resonance approximation. It is known that the variation of both the energy and the equatorial pitch-angle and, correspondingly, the significance of the pitch-angle scattering are the highest for those resonant particles which fulfill condition (4) for some integer number n giving the order of cyclotron resonance. In a homogeneous medium, the particles can be either resonant or nonresonant, depending on their longitudinal velocity. For the considered case of the

particle — wave packet interaction with varying parameters in an inhomogeneous medium, resonant conditions (4) change along the trajectory of the particle, as well as its longitudinal velocity changes. Therefore, in the situation considered the particle passes a cyclotron resonance region. In the approximation of isolated resonances, which can always be applied to the whistler wave amplitudes [20], only one slowly varying term can be kept in Hamiltonian (3), thus yielding the following form of the Hamiltonian:

$$H_n(p_\parallel, z, \mu, \varphi, t) = \frac{p_\parallel^2}{2m} + \mu\Omega(z)$$
$$+ q\Phi_0(z, t)\,J_n(\lambda) \sin\left(\Psi_0(z, t) + n\varphi\right)\,. \qquad (5)$$

The equations for the variation of the kinetic energy and the magnetic moment of the particle will have the following form in this approximation:

$$\frac{\mathrm{d}W}{\mathrm{d}t} = \frac{\omega}{n}\frac{\mathrm{d}\mu}{\mathrm{d}t} = -q\Phi_0\omega J_n(\lambda) \cos\left(\Psi_0(z, t) + n\varphi\right)\,, \qquad (6)$$

and the variations in these quantities (and, correspondingly, of the equatorial pitch-angle) during the passage through isolated cyclotron resonances will be noncorrelated.

2.2.2 Variation of the equatorial pitch-angle and the precipitation of particles into the ionosphere. As follows from formulas (4), the spacing between the resonant values of the longitudinal velocity is $\Omega/k_\parallel$. For electrons, this quantity is usually higher or close to the thermal velocity of high-energy particle distribution. Therefore, the most important resonances for electrons are the first cyclotron ($n = 1$) and the Cherenkov ($n = 0$) ones. Since the longitudinal velocities corresponding to these resonances have opposite signs, the electrons, while moving in one direction (during half of the bounce period), can resonantly interact with the wave packet when passing through only one specific resonance. As for the protons, the spacing between the resonant values of the longitudinal velocity is m_e/m_i times that for the electrons. Therefore, the protons during the half of the bounce period can interact with the wave-packet through many different cyclotron resonances.

As the analysis indicates, most of the particles — electrons and protons — are phase untrapped and the time of their interaction with the wave packet at a single resonance is determined by the generalized inhomogeneity parameter

$$\alpha_n = k_\parallel\left(\frac{\mu}{m}\frac{\mathrm{d}\omega_c}{\mathrm{d}z} + \frac{1}{2}\frac{\mathrm{d}v_{\text{res}\,n}^2}{\mathrm{d}z}\right)\,, \qquad (7)$$

and is on the order of $1/\sqrt{|\alpha|}$. In this case, it follows from equation (6) that for particles near the loss-cone boundary the variation of the equatorial pitch-angle ϑ, while passing through the cyclotron resonance, is of order

$$|\delta\vartheta| \sim \left|\frac{q\Phi_0\omega J_n(\lambda)}{W\sqrt{|\alpha|}}\right|\,. \qquad (8)$$

Expression (8) gives an estimate of the variation of the electron equatorial pitch-angle during half of their oscillation bounce period between the reflection points in opposite hemispheres. As for the protons, it was mentioned above that during half of their bounce period they can pass through many cyclotron resonances, $\Delta n \sim \omega/\Omega_{\min} \gg 1$, where $\Omega_{\min}$ is

the minimum value of the proton gyrofrequency along the line of force, for which the resonant interaction with the whistler wave becomes efficient. The value of Ω_{min} can be indirectly determined by the relations [20]

$$k_\perp(z)\,v_\perp \gtrsim \omega\,, \quad \Omega_{min} = \Omega(z)\,.$$

The transverse wave vector $k_\perp$ and the gyrofrequency $\Omega(z)$ in the quasiresonant propagation regime increase together as the distance from the equator increases. Therefore, the relations given define the minimal gyrofrequency and, consequently, the maximum number of the resonance n_{max}, for which the interaction of protons with the whistler waves is effective. The minimum number of the cyclotron resonance n_{min}, obviously, can be determined from the relation $n_{min} \sim \omega/\Omega_{max}$, where Ω_{max} is the maximum gyrofrequency of the protons along the force line, where the wave packet is situated. As was mentioned above, the variations of the equatorial pitch angle while passing through the single cyclotron resonances are noncorrelated. Therefore, the net change of the angle, which can be either positive or negative, is of the order of

$$|\Delta\vartheta| \sim \sqrt{\Delta n}\,|\delta\vartheta|\,,$$

where $|\delta\vartheta|$ is defined in expression (8), and $\Delta n = n_{max} - n_{min}$. This means that the particles, for which the value $\Delta\vartheta$ is negative and the initial equatorial pitch-angle differs from the loss-cone pitch-angle by a value less than $|\Delta\vartheta|$, fall into the loss cone and precipitate into the ionosphere.

3. Active experiments

A new line of research in the field of ionosphere–magnetosphere plasma was developed in the 1960s and was based on so-called active experiments (AEs). This line of research combined the efforts of specialists in plasma physics, radio physics, and geophysics, which helped to significantly improve our knowledge about the natural processes in the circumterresrrial plasma and also revealed a number of phenomena caused by the external influence on the magnetosphere–ionosphere system.

The results of the AEs led to discussions about the emergence of a space lab, where plasma and wave processes would be studied [1, 21, 22]. The most productive AEs were those on the influence of strong electromagnetic radiation from ground sources on the ionosphere–magnetosphere plasma. The theoretical aspects of such interaction were discussed in detail earlier in a number of papers, particularly in reviews [23, 24]. Papers [4–11] present reviews of investigations related to the influence of strong high-frequency (HF) radiation (2–12 MHz) on the ionosphere. The results of investigations concerning low-frequency (LF) radiation influence on the magnetosphere–ionosphere system are presented in monograph [12]. In Sections 3.1 and 3.2, we discuss the results of experiments which are based on direct measurements of the plasma and electromagnetic radiation parameters on board spacecraft.

3.1 Stimulated precipitation of charged particles under the action of artificial low-frequency radiation
Pitch-angle diffusion and the precipitation of charged particles from the magnetosphere to the ionosphere under the action of natural radiation is observed quite often on

satellites [25]. The first measurements of artificially stimulated precipitations were performed in an experiment with the strong LF-emitter UPD-8, operating at the 12 kHz frequency. The precipitation was registered by a modulation photometer installed aboard an airplane and directed towards the ionosphere above the emitter [27]. As the emitter was turned on, an increase in the luminosity of the night sky of ≈ 40 Rl was observed at the wavelength $\lambda = 3.914 \times 10^{-7}$ m. This is the line of excited nitrogen, and therefore its intensity is proportional to the precipitating particle flux density. Estimations of the total energy flux give the value of 0.13 erg cm^{-2} s^{-1}, which corresponds to an electron flux of 5×10^6 cm^{-2} s^{-1} with an energy of 15 keV.

Direct measurements of stimulated precipitations were performed on the satellite *Arkad-3* together with the LF-emitter UPD-8 [28], which was a source of an amplitude-modulated signal at the 15 kHz frequency. As the satellite passed at the altitude of 1500–2000 km above the emitter, fluxes of electrons with energies of 0.6–2 keV increased from 5×10^3 cm^{-2} s^{-1} (noise level in this experiment) to 2.5×10^4 cm^{-2} s^{-1}.

A similar experiment was performed in the USA on the S81-1 satellite as it passed over an NAA (National Aeronautic Association) emitter [29]. During the experiment, an increase in the electron flux intensity was detected at energies of $E > 6$ keV up to the value of 10^3 cm^{-2} s^{-1}. It should be noted that the NAA emitter is located at mid-latitudes ($L = 3.2$), and the UPD-8 is located more to the north at subauroral ($L = 4.0$) latitudes. The difference in the flux intensities of the precipitating electrons can be explained not only by different geomagnetic conditions but also by the difference in the trapped particle density at different latitudes. Subsequent measurements on the *DEMETER* (Detection of Electro-Magnetic Emissions Transmitted from Earthquake Regions) satellite confirmed these results [30].

The first measurements of precipitating proton fluxes stimulated by artificial low-frequency radiation were performed on the *Arkad-3* satellite. Figure 1 shows the results of these measurements.

The intensity of proton fluxes with an energy of 110 keV becomes 2.5 times higher for optimal observation condi-
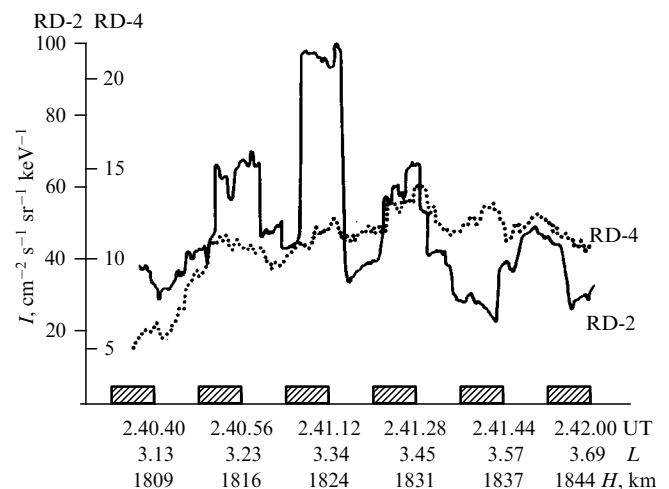

Figure 1. Intensity variation of proton fluxes with energies of ≈ 110 keV (curve RD-2) and ≈ 190 keV (curve RD-4) as the *Arkad-3* satellite passed over the UPD-8 emitter (taken from Ref. [31]). The time intervals when the emitter was operating are marked by rectangles.

tions — magnetic coupling with the ionosphere above the emitter. In this case, the fluxes of protons with higher energy (190 keV) change insignificantly around the noise level. It should be noted that in different measurement series the stimulated flux intensity of the precipitating protons varied from 80 to 500 $cm^{-2}\,s^{-1}$, depending on the geomagnetic activity, which may be related to the density of the trapped particles.

Summing up, measurements of the particle fluxes as the satellite passed over the low-frequency ground emitter resulted in:

— precipitating electron fluxes with an intensity of $\approx 10^3 - 10^4\ cm^{-2}\,s^{-1}$;

— precipitating proton fluxes with an energy of ≈ 110 keV. The intensity of the proton fluxes was $80 - 500\ cm^{-2}\,s^{-1}$.

The mechanism of the proton precipitation under the action of the signal from a very low-frequency (VLF) emitter, suggested in paper [20], is similar to the mechanism of proton precipitation stimulated by lightning discharge radiation, which was discussed in Section 2.

3.2 Formation of inhomogeneities stretched along the magnetic field due to low-frequency heating

It was shown in paper [32] that a significant amount of the energy of electromagnetic waves from the low-frequency band goes into the local heating of the ionosphere. During the daytime hours in the summer, these losses can reach 90%. Therefore, the radiation from powerful ground LF-emitters influences the ionosphere in a similar way as the HF-heating facilities [4–11].

Experimental investigations of ionosphere heating under the action of artificial LF-radiation were performed on the *Arkad-3* satellite [33]. Figure 2 depicts the measurement results for the fluxes of three different cold ionosphere ions and for the electromagnetic field when passing over the LF-emitter.

The fluxes of the upgoing ions are maximal when the intensity of the emitted electromagnetic field is maximal (at 15 kHz frequency). The change in the radiation intensity at the frequency of 4.5 kHz (in the vicinity of the local frequency for the lower hybrid resonance (LHR)) indicates the ion heating mechanism is related to LHR-radiation, which is confirmed by the theoretical predictions in monograph [12].

The heating of the ionosphere plasma under the action of HF-radiation leads to particle transport from the ionosphere to the magnetosphere and to the formation of ducts — plasma inhomogeneities stretched along the magnetic field [34, 35]. In a similar way, the ducts can be formed during LF-heating [36, 37].

We should note that some of the problems concerning the duct formation under the action of strong radio emission are still unsolved. Particularly, there is still no theoretical explanation for the fast process of ionosphere plasma reaching heights of several Earth radii [38].

Summing up, the plasma inhomogeneities stretched along the magnetic field can be formed above the low-frequency emitters in two ways:

— as a result of ionosphere plasma heating by LF-radiation;

— as a result of the stimulated precipitation of high-energy particles and the formation of the region with an enhanced ionization.
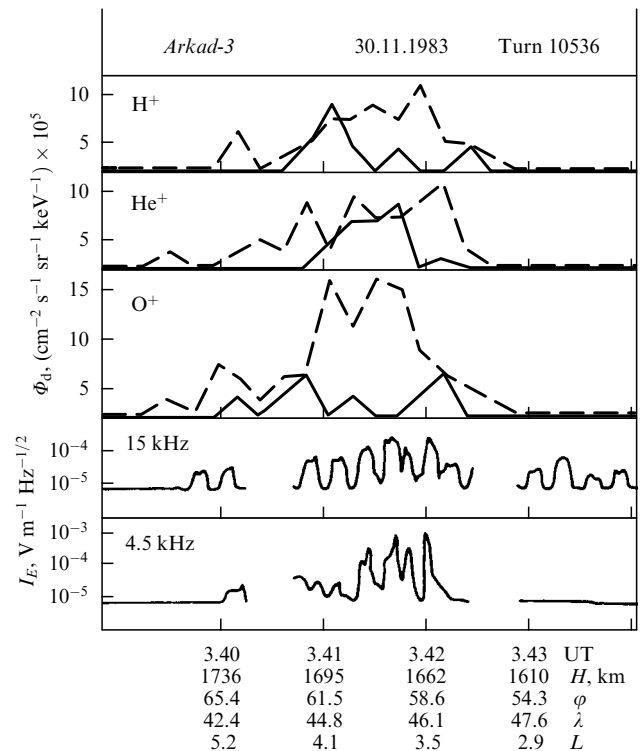

Figure 2. Differential fluxes Φ_d of the hydrogen, helium, and oxygen ions (three upper plots) and the intensity I_E of electromagnetic radiation at 15 and 4.5 kHz frequencies (two lower plots), measured on the *Arkad-3* satellite as it passed over an LF-emitter (taken from Ref. [33]). Solid and dashed lines correspond to two directions of measuring the ion arrival.

The first mechanism is most effective during the daytime in the summer, while the second one is best during the nighttime in winter.

4. Conclusions

Theoretical investigations, as well as ground and aboard spacecraft measurements of ionosphere–magnetosphere system parameters have allowed us to obtain an almost complete picture of the dynamical processes in the circumterrestrial plasma. However, a number of key questions remain unanswered: the mechanism of ionosphere ion heating under the action of HF-radiation is not fully understood, the characteristics of ionosphere ion transport to great altitudes are unknown, etc. The Rezonans space project should give answers to these and other relevant questions [38].

In the Rezonans mission, two pairs of satellites will be launched into specially selected orbits, which will allow performing long (up to tens of minutes) measurements of the plasma and electromagnetic field parameters in the chosen magnetic field tube, which has its footprint in the ionosphere above the radiation source. Such an experimental configuration will allow us to investigate the dynamics of processes caused by artificial electromagnetic radiation.

References

1. Artsimovich L A, Sagdeev R Z *Fizika Plazmy dlya Fizikov* (Plasma Physics for Physicists) (Moscow: Atomizdat, 1979)
2. Lauben D S, Inan U S, Bell T F *J. Geophys. Res.* **106** 29745 (2001)
3. Shklyar D R, Kuzichev I V *Geophys. Res. Lett.* **41** 201 (2014)
4. Gurevich A V *Phys. Usp.* **50** 1091 (2007); *Usp. Fiz. Nauk* **177** 1145 (2007)
5. Frolov V L et al. *Phys. Usp.* **50** 315 (2007); *Usp. Fiz. Nauk* **177** 330 (2007)
6. Gurevich A V *Sov. Phys. Usp.* **17** 613 (1975); *Usp. Fiz. Nauk* **113** 728 (1974)
7. Shlyuger I S *Sov. Phys. Usp.* **17** 613 (1975); *Usp. Fiz. Nauk* **113** 729 (1974)
8. Vas'kov V V, Gurevich A V *Sov. Phys. Usp.* **17** 614 (1975); *Usp. Fiz. Nauk* **113** 730 (1974)
9. Belikovich V V et al. *Sov. Phys. Usp.* **17** 615 (1975); *Usp. Fiz. Nauk* **113** 732 (1974)
10. Grach S M et al. *Sov. Phys. Usp.* **17** 616 (1975); *Usp. Fiz. Nauk* **113** 734 (1974)
11. Shvartsburg A B *Sov. Phys. Usp.* **17** 617 (1975); *Usp. Fiz. Nauk* **113** 735 (1974)
12. Molchanov O A *Nizkochastotnye Volny i Indutsirovannye Izlucheniya v Okolozemnoi Plazme* (Low-Frequency Waves and Induced Radiation in Near-Earth Plasma) (Moscow: Nauka, 1985)
13. Christian H J et al. *J. Geophys. Res.* **108** 4005 (2003)
14. Collier A B et al. *J. Geophys. Res.* **116** A03219 (2011)
15. Al'pert Ya L *Usp. Fiz. Nauk* **60** 369 (1956)
16. Al'pert Ya L *Sov. Phys. Usp.* **9** 787 (1967); *Usp. Fiz. Nauk* **90** 405 (1966)
17. Colman J J, Starks M J *J. Geophys. Res.* **118** 4471 (2013)
18. Parrot M et al. *J. Geophys. Res.* **113** A11321 (2008)
19. Alekhin Yu K, Shklyar D R *Geomagn. Aeronomiya* **20** 501 (1980)
20. Shklyar D R *Planet. Space Sci.* **34** 1091 (1986)
21. Genkin L G, Erukhimov L M *Phys. Rep.* **186** 97 (1990)
22. Markov G A, Belov A S *Phys. Usp.* **53** 703 (2010); *Usp. Fiz. Nauk* **180** 735 (2010)
23. Ginzburg V L, Gurevich A V *Sov. Phys. Usp.* **3** 115 (1960); *Usp. Fiz. Nauk* **70** 201 (1960)
24. Ginzburg V L, Gurevich A V *Sov. Phys. Usp.* **3** 175 (1960); *Usp. Fiz. Nauk* **70** 393 (1960)
25. Rosenberg T J, Helliwell R A, Katsufrakis J P *J. Geophys. Res.* **76** 8445 (1971)
26. Zhulin I A et al. *Sov. Phys. Dokl.* **21** 579 (1976); *Dokl. Akad. Nauk SSSR* **230** 1073 (1976)
27. Lyakhov S B, Managadze G G *Prib. Tekh. Eksp.* (3) 200 (1975)
28. Kovrazhkin R A et al. *JETP Lett.* **38** 397 (1983); *Pis'ma Zh. Eksp. Teor. Fiz.* **38** 332 (1983)
29. Imhof W L et al. *Geophys. Res. Lett.* **10** 361 (1983)
30. Sauvaud J-A et al. *Geophys. Res. Lett.* **35** L09101 (2008)
31. Kovrazhkin R A et al. *JETP Lett.* **39** 228 (1984); *Pis'ma Zh. Eksp. Teor. Fiz.* **39** 193 (1984)
32. Aksenov V I et al. *Radiophys. Quantum Electron.* **18** 985 (1975); *Izv. Vyssh. Ucheb. Zaved. Radiofiz.* **18** 1333 (1975)
33. Dzhordzhio N V et al. *JETP Lett.* **46** 405 (1987); *Pis'ma Zh. Eksp. Teor. Fiz.* **46** 322 (1987)
34. Frolov V L et al. *JETP Lett.* **88** 790 (2008); *Pis'ma Zh. Eksp. Teor. Fiz.* **88** 908 (2008)
35. Milikh G M et al. *Geophys. Res. Lett.* **35** L17104 (2008)
36. Milikh G M et al. *Geophys. Res. Lett.* **37** L07803 (2010)
37. Mogilevsky M M et al. *Cosmic Res.* **52** 68 (2014); *Kosmich. Issled.* **52** (1) 71 (2014)
38. Mogilevsky M M et al., in *Dynamics of the Earth's Radiation Belts and Inner Magnetosphere* (Geophysical Monograph, Vol. 199, Eds D Summers et al.) (Washington, DC: American Geophysical Union, 2012) p. 117